The endocranial shape of *Australopithecus africanus*: surface analysis of the endocasts of Sts 5 and Sts 60

Amélie Beaudet,[1,2,*] Jean Dumoncel,[3,4] Frikkie de Beer,[5] Stanley Durrleman,[6] Emmanuel Gilissen,[7,8] Anna Oettlé,[2,9] Gérard Subsol,[10] John Francis Thackeray[11] and José Braga[3,11]

[1]School of Geography, Archaeology and Environmental Studies, University of the Witwatersrand, Johannesburg, South Africa
[2]Department of Anatomy, University of Pretoria, Pretoria, South Africa
[3]Laboratoire d'Anthropologie Moléculaire et Imagerie de Synthése, UMR 5288 CNRS-Université de Toulouse (Paul Sabatier), Toulouse Cedex, France
[4]Institut de Recherche en Informatique de Toulouse, UMR 5505 CNRS-Université de Toulouse (Paul Sabatier), Toulouse Cedex, France
[5]Radiation Science Department, South African Nuclear Energy Corporation (Necsa), Pelindaba, South Africa
[6]Institut du Cerveau et de la Moelle épinière, Aramis Team, INRIA Paris, Sorbonne Universités, UPMC Université Paris 06 UMR S 1127, Inserm U 1127, CNRS UMR 7225, Paris, France
[7]Department of African Zoology, Royal Museum for Central Africa, Tervuren, Belgium
[8]Laboratory of Histology and Neuropathology, Université Libre de Bruxelles, Brussels, Belgium
[9]Department of Anatomy and Histology, Sefako Makgatho Health Sciences University, Pretoria, South Africa
[10]Montpellier Laboratory of Informatics, Robotics and Microelectronics, UMR 5506 CNRS, Université de Montpellier, Montpellier, France
[11]Evolutionary Studies Institute and School of Geosciences, University of the Witwatersrand, Johannesburg, South Africa
*Correspondence: A. Beaudet, School of Geography, Archaeology and Environmental Studies, University of the Witwatersrand, 1 Jan Smuts Avenue, Braamfontein, Johannesburg 2000, South Africa.
E: beaudet.amelie@gmail.com

Abstract

Assessment of global endocranial morphology and regional neuroanatomical changes in early hominins is critical for the reconstruction of evolutionary trajectories of cerebral regions in the human lineage. Early evidence of cortical reorganization in specific local areas (e.g. visual cortex, inferior frontal gyrus) is perceptible in the non-human South African hominin fossil record. However, to date, little information is available regarding potential global changes in the early hominin brain. The introduction of non-invasive imaging techniques opens up new perspectives for the study of hominin brain evolution. In this context, our primary aim in this study is to explore the organization of the *Australopithecus africanus* endocasts, and highlight the nature and extent of the differences distinguishing *A. africanus* from the extant hominids at both local and global scales. By means of X-ray-based imaging techniques, we investigate two *A. africanus* specimens from Sterkfontein Member 4, catalogued as Sts 5 and Sts 60, respectively a complete cranium and a partial cranial endocast. Endocrania were virtually reconstructed and compared by using a landmark-free registration method based on smooth and invertible surface deformation. Both local and global information provided by our deformation-based approach are used to perform statistical analyses and topological mapping of inter-specific variation. Statistical analyses indicate that the endocranial shape of Sts 5 and Sts 60 approximates the *Pan* condition. Furthermore, our study reveals substantial differences with respect to the extant human condition, particularly in the parietal regions. Compared with *Pan*, the endocranial shape of the fossil specimens differs in the anterior part of the frontal gyri.

Key words: deformation-based models; endocast; hominin; paleoneurology; Sterkfontein

Introduction

Tracking the early emergence of the derived *Homo*-like neuroanatomical features in the hominin fossil record can be expected to contribute to an understanding of the timing and mode of critical endocranial changes (i.e. size and cortical reorganization). Together with studies of comparative neuroanatomy in extant mammal taxa (Barton & Harvey, 2000; Gómez-Robles et al. 2014) and quantitative genetic analyses (Hager et al. 2012), the early hominin fossil record may provide evidence of a 'mosaic-like' evolution of cerebral features commonly regarded as typical of extant humans (Holloway, 2001). For instance, the presumed caudal position of the lunate sulcus in the endocast of the holotype of *Australopithecus africanus* (i.e. the Taung child; Dart, 1925; Holloway, 1981) illustrates potentially early (i.e. pre-*Homo*) changes in the configuration of the occipital lobes, likely indicative of an expansion of parietal association cortex. Similarly, the original description of the endocast of *Australopithecus sediba* (i.e. MH1) reveals that the reorganization of the prefrontal cortex was initiated at least 1.9 million years ago and occurred before brain size expansion (Carlson et al. 2011). However, the position of the lunate sulcus in the Taung child, as well as in other South African specimens (e.g. StW 505), is still highly controversial (Falk, 1980, 1983a, 2009; Holloway, 1981; Holloway et al. 2004a). Additionally, an alternative hypothesis suggests a global reorganization of the hominin brain (i.e. concerted evolution of the brain; Finlay & Darlington, 1995; de Winter & Oxnard, 2001; Falk, 2009).

The *Homo* fossil record yields further evidence of the complexity of hominin brain evolution. Besides depicting fundamental non-allometric brain shape changes involving overall neurocranial organization (e.g. globularization process; Lieberman et al. 2002; Gunz et al. 2010; Neubauer et al. 2010), it confirms that an increase in brain size is not a prerequisite for cerebral reorganization (see fig. 4: Holloway, 1983) or for the emergence of human-like neuroanatomical features. Indeed, specimens attributed to various fossil species of *Homo* (e.g. *Homo erectus*, *Homo floresiensis*, *Homo naledi*) combine an australopith-like cranial capacity with human-like sulcal organization (e.g. horizontal and ascending rami of the Sylvian fissure in the lateral prefrontal cortex, caudal position of the lunate sulcus; Gabunia et al. 2000; Brown et al. 2004; Falk et al. 2005; Lee, 2005; Grimaud-Hervé et al. 2006; Kubo et al. 2013; Lordkipanidze et al. 2013; Berger et al. 2015; Holloway et al. 2017; Hurst et al. 2017). Accordingly, the assessment of global endocranial morphology (e.g. globularization) and regional neuroanatomical changes (e.g. topographic reduction of the visual cortex and expansion of the prefrontal cortex) are critical for the reconstruction of the evolutionary trajectories of cerebral regions in the human lineage and understanding underlying reorganizational processes.

Assessing early hominin brain evolution is, however, significantly hampered by both technical limitations and the fragmentary nature of fossil endocasts, notwithstanding previous exhaustive descriptive studies (Holloway, 1972, 1981, 1983; Falk, 1980, 1983b; Tobias, 1991; Holloway et al. 2004b). Early attempts to quantitatively characterize early hominin endocranial shape have stressed the need of analytical tools providing "the critical 'localness' to compare regions between taxa in any objective, statistically significant way" (Holloway, 1980: p. 201). Original applications of imaging techniques revealed the potential of non-invasive investigation of early hominins specimens, particularly from the rich South African fossil record (Conroy et al. 1990, 1998; Spoor et al. 2000). In this context, the

integration of radiation-based high-resolution three-dimensional (3D) methods in the traditional investigative toolkit of paleoneurology discloses new perspectives for tracking the potential covariation patterns in fossil endocranial morphoarchitecture. As, for instance, shape analysis in extant hominids provided critical information for intra-specific cerebral variation (Gilissen, 2001). More specifically, the landmark-free deformation-based models have been demonstrated to be a relevant tool for the registration of morphoarchitectural variations in primate endocranial ontogenetic trajectories (Durrleman et al. 2012a), and also for taxonomic and evolutionary studies in fossil primate taxa (Beaudet et al. 2016a; Beaudet & Bruner, 2017).

As highlighted in previous paleoneurological studies, mostly because of their preservation state, the *A. africanus* specimens Sts 5 and Sts 60, respectively, a complete cranium and a partial cranial endocast, are critical for understanding early hominin brain changes (Falk et al. 2000; Holloway et al. 2004b; Neubauer et al. 2012). Indeed, Holloway et al. (2004b) stated that "This [Sts 60] is one of the best of the five natural brain endocasts that exist for the South African gracile forms in terms of sulcal markings, and size estimation." (p. 77) and "Despite the preceding judgments, the endocast [of Sts 5] is complete, relatively undistorted, and provides an accurate endocranial volume […]" (p. 73). Accordingly, our primary aim in this study was to explore at both global and local scales the endocranial organization in Sts 5 and Sts 60, and provide formal (statistical) comparisons with extant hominids using the deformation-based models. Besides using classical protocols in deformation-based surface comparison (Dumoncel et al. 2014; Beaudet et al. 2016a,b; Beaudet & Bruner, 2017), we also applied the recently developed deformation-based method for estimating and dealing with missing parts in incomplete specimens (Dumoncel et al. 2016), as our sample included complete (Sts 5) and partial (Sts 60) endocasts.

Materials and methods

The fossil specimens investigated in our study included two *A. africanus* representatives, Sts 5 and Sts 60, both derived from Sterkfontein Member 4. They are currently curated at the Ditsong National Museum of Natural History (Pretoria, South Africa). The specimen Sts 5, or 'Mrs Ples', is a well-preserved cranium, suggested by Broom (1947) to be an adult female. This specimen lacks only a small neurocranial portion that was physically filled using reconstruction material (Fig. 1a). Sts 60, on the other hand, is a natural partial endocast preserving most of the left side, excluding some parts of the frontal and temporal poles, the entire occipital pole as well as the posterior cerebellar lobe, while the right side is represented only by the frontal lobe and a portion of the parietal lobe (Fig. 1a; Broom & Schepers, 1946; Holloway et al. 2004b). The right hemisphere of the original specimen, as well as the occipital and cerebellar lobes and the foramen magnum region, has been reconstructed with plaster (Fig. 1a). Sts 60 is associated to the severely crushed cranium TM 1511. Sts 5 and Sts 60 have been described as relatively undistorted (Holloway et al. 2004a). The cranium of Sts 5 was scanned by a medical scanner with a spatial resolution of 0.35 × 0.35 × 0.2 mm at the Little Company of Mary Hospital (Pretoria). The external surface of Sts 60 was digitally captured by the surface scanner NextEngine 3D Scanner Ultra HD with an isometric resolution of 0.2 mm (Fig. 1a).

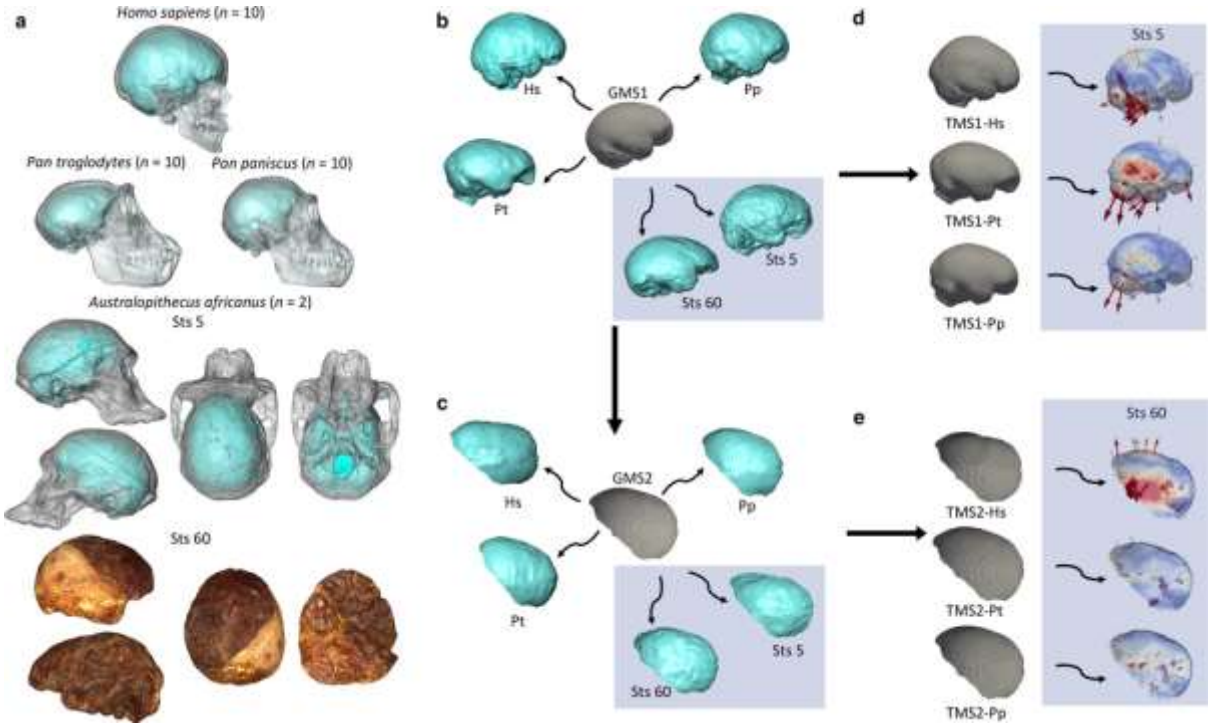

Figure 1. Virtual endocasts and computation process. Digital reconstruction of crania (light grey) and endocasts (blue) in a human, a common chimpanzee and a bonobo, and in the *Australopithecus* specimens Sts 5 and Sts 60 (a). Plaster used to reconstruct the endocast of Sts 60 corresponds to the lighter surface. Computation process consists successively in the deformation of a global mean shape (GMS1) to complete endocasts of the extant specimens and the subsequent inclusion of the fossil specimens (blue square) (b); the deformation of a second global mean shape (GMS2) to partial endocasts of the extant specimens (i.e. the regions corresponding to the missing part in Sts 60 were removed from the complete endocasts of the extant specimens and Sts 5 based on the results of the first deformation process) and subsequent inclusion of the fossil specimens (blue square) (c). Taxon mean shapes (TMS) are generated from complete (d) and partial (e) endocasts and subsequently deformed to Sts 5 and Sts 60, respectively (blue squares). Topographical distribution of displacements is rendered by colour maps (d,e). Complete and partial endocasts are represented in lateral (b,d) and superior (c,e) views, respectively.

As comparative material, we investigated three samples representing *Homo sapiens* (*n*= 10), *Pan troglodytes* (*n*= 10) and *Pan paniscus* (*n* = 10), with equal proportions of fully mature males and females. Extant humans were selected from anonymized human clinical records of the Pasteur Hospital in Toulouse, France (El Khoury et al. 2014). The patients were scanned by medical computed-tomography (CT) with a spatial resolution ranging between 0.49 and 0.50 mm. Common chimpanzee and bonobo specimens from the Royal Museum for Central Africa (Tervuren, Belgium) were imaged using medical CT with a spatial resolution ranging between 0.39 and 0.8 mm (El Khoury et al. 2014).

The digital extraction and reconstruction of Sts 5 and the extant hominid endocrania were automatically performed through the Endex software (Fig. 1a; http://liris.cnrs.fr/gilles.gesquiere/wiki/doku.php?id=endex; Subsol et al. 2010). Endocrania were compared by using a size-independent and landmark-free registration method based on smooth and invertible surface deformation (Durrleman, 2010; Durrleman et al. 2012a,b; Dumoncel et al. 2014; Beaudet et al. 2016a,b). As a pre-processing step, the surfaces were automatically aligned in position, orientation and scale with respect to one surface randomly selected using the Iterative Closest Point algorithm (Besl & McKay, 1992). From

this set of pre-aligned surfaces, an automatic non-rigid registration process was performed on the extant specimens only (i.e. *Homo* and *Pan* samples) via the deformation of a template using the software Deformetrica (http://www.deformetrica.org/; Durrleman, 2010; Beaudet et al. 2016a; Fig. 1b). This process provided an atlas (*sensu* Durrleman et al. 2014), i.e. a global mean shape (GMS1) and the deformation fields from the global mean shape to each extant specimen, and is called hereinafter STEP 1. From STEP 1, taxon mean shapes (TMS1-Hs, TMS1-Pp and TMS1-Pt) were generated (Fig. 1b,d; Beaudet et al. 2016a). Finally, GMS1 was subsequently deformed to Sts 5 and Sts 60, thus providing the deformation fields from GMS1 to each fossil specimen (Fig. 1b,d; Beaudet et al. 2016a). Similarly, TMS1-Hs/TMS1-Pp/TMS1-Pt were deformed to Sts 5 and Sts 60.

Because the original natural endocast of Sts 60 is incomplete, we computed a second analysis (STEP 2) focusing on the preserved endocranial region in Sts 60 following the protocol published in Dumoncel et al. (2016). Firstly, we virtually and manually removed the artificial endocranial region following the physical limit between the natural endocast and the material used for reconstructing the missing part (Fig. 1a). Based on the results of STEP 1 and by using the deformations between GMS1 and Sts 60, as well as the deformations between GMS1 and each specimen (including Sts 5), the region corresponding to the missing surface in Sts 60 was similarly removed from each endocast (Dumoncel et al. 2016; Fig. 1c). Then, we computed a second atlas, including a second global mean shape (GMS2), from the set of partial endocasts. Taxon mean shapes (TMS2-Hs, TMS2-Pp and TMS2-Pt; Fig. 1c,e) were generated. As for the analysis of the complete endocasts, GMS2 was deformed to the partial endocasts of Sts 5 and Sts 60, thus providing the deformation fields from GMS2 to each fossil specimen (Fig. 1c,e). Additionally, TMS2-Hs/TMS2-Pp/TMS2-Pt were deformed to Sts 5 and Sts 60.

The deformation fields integrating local orientation and the amplitude of the deformations from the GMS1 and GMS2 to each specimen were statistically analysed by between-group principal component analysis (bgPCA; Mitteroecker & Bookstein, 2011) using the package ade4 for R (Dray & Dufour, 2007). Based on the covariance matrix of the predefined extant group means, the fossil specimens were subsequently projected into the shape space of the two analyses. Accordingly, we computed two separate bgPCAs, i.e. a first one with the complete endocasts (excluding Sts 60), and a second one with the partial endocasts (including both Sts 5 and Sts 60).

The amplitude and orientation of the displacements recorded during the deformation process were rendered by a combination of colour maps and vectors. Vectors represent the local maxima (i.e. the vectors for which the norm is superior to all of the norms recorded for its nearest neighbours) of the displacements. Colour maps were computed for the comparison between TMS1-Hs/TMS1-Pp/TMS1-Pt and Sts 5, and between TMS2-Hs/TMS2-Pp/TMS2-Pt and Sts 60 (Fig. 1d,e).

Results

Based on the deformations computed from the extant hominid groups to the virtual endocasts of Sts 5 and Sts 60 using both complete and partial endocasts, statistical analyses indicate that the morphology in these two *A. africanus* endocranial specimens closely approximates the *Pan* condition along the two bgPCs (Fig. 2). However, Sts 60 plots within the non-human groups, while Sts 5 falls outside the *Pan* variation as represented by the convex hulls in both analyses (Fig. 2). Moreover, according to the bgPCA and the position of the specimen in the shape space, the morphology of the Sts 5 endocast is closer to *Pan* when considering the overall shape (Fig. 2a) than in the analysis of partial endocasts (Fig. 2b).

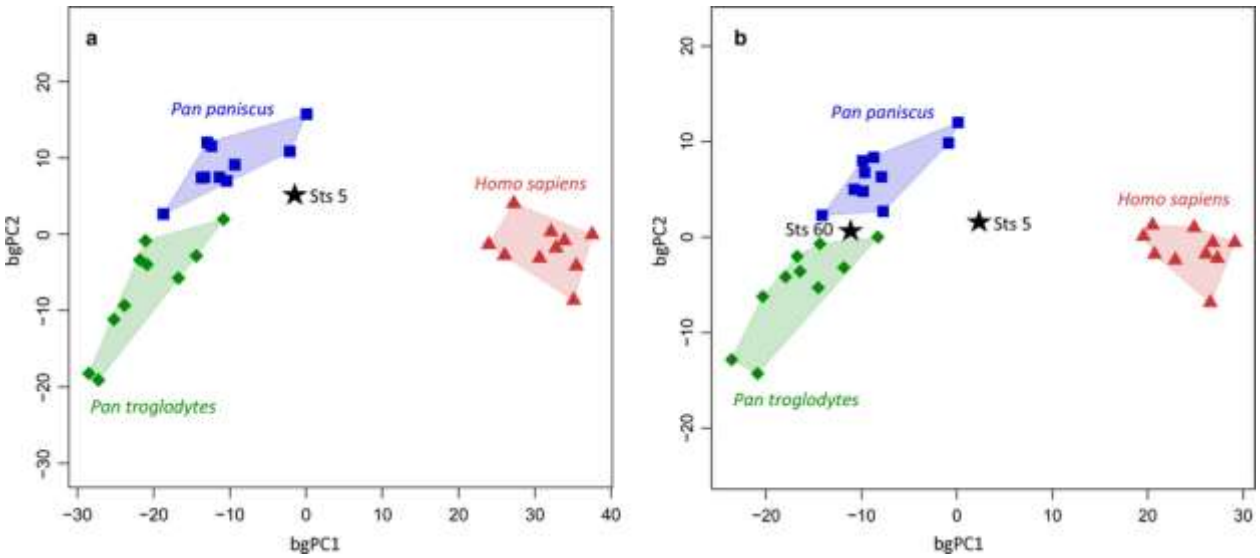

Figure 2. Statistical analyses of the endocranial shape comparison. Between-group principal component analysis (bgPCA) of the deformation-based shape comparisons of the complete (a) and partial (b) endocasts extracted from *Australopithecus* (black stars), extant humans (red triangles), common chimpanzees (green diamonds) and bonobos (blue squares).

We investigated the nature and extent of the differences distinguishing Sts 5 and Sts 60 from extant *Homo* and *Pan* representatives based on topological mapping of inter-specific variation of complete and incomplete endocasts, respectively (Fig. 3). Compared with extant humans, the dorsal part of the parietal lobes is more flattened in both Sts 5 and Sts 60, and the occipital lobes are less protruded in Sts 5. According to the vectors, Sts 60 experienced larger deformation on top of the endocast in terms of magnitude than Sts 5. The well-preserved left temporal lobe of Sts 60 is more inflated, while in Sts 5 the precentral gyri in both hemispheres are more prominent. The frontal bec is more elongated and the orbital surfaces are more elevated in the fossil specimens.

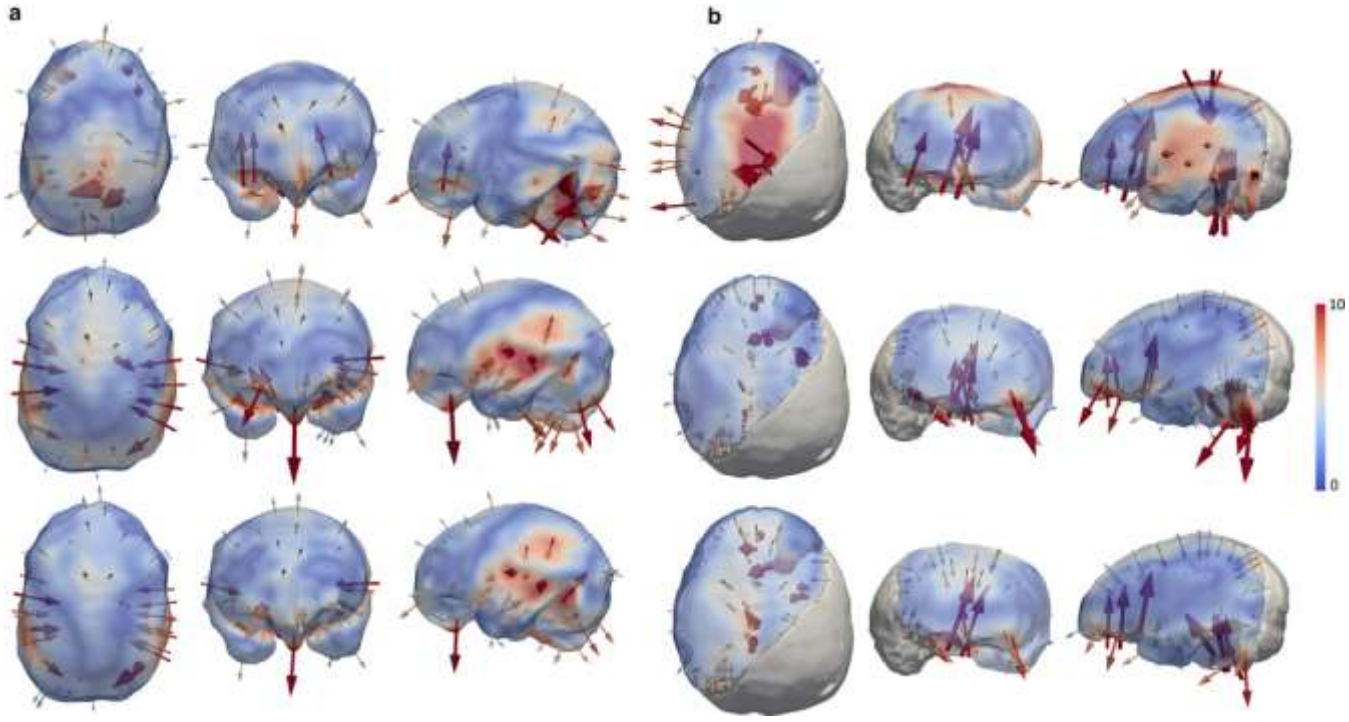

Figure 3. Topographical distribution of morphological deformations. Comparative maps of morphological deformations from the taxon mean shapes (TMS) computed for the extant human (top row), common chimpanzee (middle row) and bonobo (bottom row) samples, to Sts 5 (a) and Sts 60 (b). While the overall endocast of Sts 5 is analysed, in Sts 60 shape comparison is limited to the well-preserved partial endocast, accordingly the reconstructed part (in grey) is excluded from the computation process. Endocasts are shown in superior, anterior and lateral (left) views. Cumulative displacement variations are rendered by a pseudo-colour scale ranging from dark blue (lowest values) to red (highest values) at the individual surfaces and vectors. The vectors represent both the magnitude and orientation of the deformations from the TMS to the fossil specimens. The maximum value of the colour bar (10) is considered to be the most appropriate compromise representation of both global and local deformations, even if some recorded deformations exceeded this value. For each view, the hidden side of the endocranial surface was virtually removed. A description of the main morphological variations is provided in the text.

Compared with *Pan*, the frontal bec in Sts 5 is more developed and the biparietal width is narrower. The configuration of the notch forming the junction between the temporal lobe and the cerebellar area in the lateral surface differs in Sts 5 as compared with *Pan* by combining a medial indentation with a caudal elongation of the temporal lobe. Additionally, the ventral surface of the frontal lobes in Sts 60 is more elevated. In both *Australopithecus* specimens, the cerebellar lobes and the anterior regions of the frontal gyri are more protuberant when compared with *Pan*. On the whole, the region surrounding the foramen magnum is more protruded in Sts 5 and less developed in Sts 60 in comparison to the extant taxa.

Discussion

Our results reveal that the *A. africanus* endocranial morphology represented by Sts 5 and Sts 60 is closer to the non-human condition, which is consistent with previous landmark-based morphometric investigation of the two specimens (Neubauer et al. 2012). However, while the landmark-based study essentially described general patterns of rounded vs. elongated endocranial shapes, here we suggest additional characteristics, including a more

elongated frontal bec and a substantially less elevated parietal area in Sts 5 and Sts 60 compared with *Homo*. The last feature is consistent with the late emergence in the hominin lineage of the parietal expansion that contributed to the globular shape of the extant human brain (Bruner et al. 2003).

Changes are perceptible in the anterior part of the prefrontal cortex (lateral and ventral) in both Sts 5 and Sts 60 as compared with the *Pan* specimens. These results should be considered cautiously as the degree of preservation of the Sts 5's cranium and of the Sts 60's natural endocast at this level is not optimal (Holloway et al. 2004b). Nonetheless, these changes might be consistent with the reconfiguration of the orbito-frontal region described in *Australopithecus* endocasts as compared with the putative ape-like ancestral pattern (Falk, 2009, 2012; Carlson et al. 2011) or with other early hominin taxa (e.g. *Paranthropus*; Falk et al. 2000). However, the detection of potential prefrontal cortical changes should be supported by further analysis of the sulcal pattern that may be indicative of the spatial organization of crucial cortical areas such as the Broca's cap (for review, see Falk, 2014), within the limits of neuroanatomical inferences (Amunts et al. 1999). Moreover, a larger sample of *Australopithecus* specimens will be necessary for confirming (or rejecting) the morphological changes observed, analysed and reported in this study.

On the contrary, the substantial protrusion of the cerebellum in both Sts 5 and Sts 60 and the narrower biparietal width in Sts 5 observed when compared with *Pan* is more difficult to explain. Additionally, while previous studies suggested a chimpanzee-like configuration of the basicranial shape in Sts 5, and more particularly of the petrous pyramid (Spoor, 1997), we found differences with *Pan* in the petrosal region. Besides the fact that the proxy commonly used for representing the ancestral morphotype (i.e. the panins) is probably not a reliable ancestral equivalent for every aspect of the hominin brain, one possible explanation to consider is the presence of cerebral traits specific to *A. africanus*. Moreover, the neuro-basicranial complex is a highly integrated morphological unit, and the intimate relationship between the two components adds another confounding factor when interpreting cerebral changes from the endocranial shape (Lieberman et al. 2000).

In our study, morphological affinities of Sts 5 with the extant hominoid groups as revealed by the shape comparison slightly vary whether or not we integrate the occipital lobes, right temporal lobe and a portion of the parietal region. This result might be affected by the intra-specific variation within the comparative groups or may potentially suggest that some of the morphological features excluded in the analysis of partial endocasts could be relevant for interpreting morphological differences between *Australopithecus* and extant hominids. Furthermore, Sts 60 differs from Sts 5, notably by displaying a more flattened dorsal portion of the parietal lobes. This result may be potentially compatible with possible post mortem supero-inferior compression evidenced by the landmark-based geometric morphometric analysis performed by Neubauer et al. (2012) and consistent with the preservation state of the associated crushed cranium TM 1511 (Broom & Schepers, 1946). Additionally, portions of the frontal and left temporal poles are missing in Sts 60 and should be considered in the interpretations of surface comparison described in this paper. In the future, the complete reconstruction of this specimen based on extant (i.e. human, chimpanzee, bonobo) models, including the correction of potential plastic distortion (Tallman et al. 2014), should be a priority.

Acknowledgements

The authors thank Stephany Potze, curator of the Palaeontology Section of the Ditsong National Museum of Natural History (Pretoria), the Little Company of Mary Hospital (Pretoria) and Benjamin Moreno (Toulouse) for collection access and data acquisition. Model-based deformation computation was granted access to the HPC resources of CALMIP (Grant 2016-P1440). For scientific contributions and/or discussion, the authors are especially grateful to M.C. Bosman (Pretoria), E. Bruner (Burgos), R. Macchiarelli (Poitiers & Paris), A. van Schoor (Pretoria) and C. Zanolli (Toulouse). The present version greatly benefited from the comments provided by three anonymous reviewers. This research has been supported by the AESOP+ program, the Center of Research and Higher Education (PRES) of Toulouse, the Midi-Pyrénées Region, the French Ministry of Foreign Affairs, the National Center for Scientific Research (CNRS), the National Research Foundation of South Africa (NRF) and the Department of Science and Technology (DST) of South Africa. The support of the Claude Leon Foundation and the DST-NRF Centre of Excellence in Palaeosciences (CoE-Pal) towards this research is hereby acknowledged. Opinions expressed and conclusions arrived at, are those of the author and are not necessarily to be attributed to the CoE. The authors declare no conflict of interest.

Author's contributions

AB designed research, performed data analysis/interpretation and drafting of the manuscript; JD contributed new analytical tools, data analysis and critical revision of the manuscript; FdB, SD, EG, AO, GS and FT provided critical revision of the manuscript and approval of the article; JB designed research, contributed acquisition of CT data and provided critical revisions of the manuscript.

References

Amunts K, Schleicher A, Bürgel U, et al. (1999) Broca's region revisited: cytoarchitecture and intersubject variability. *J Comp Neurol* 412, 319–341.

Barton RA, Harvey PH (2000) Mosaic evolution of brain structure in mammals. *Nature* 405, 1055–1058.

Beaudet A, Bruner E (2017) A frontal lobe surface analysis in three archaic African human fossils: OH 9, Buia, and Bodo. *C R Palevol* 16, 499–507.

Beaudet A, Dumoncel J, de Beer F, et al. (2016a) Morphoarchitectural variation in South African fossil cercopithecoid endocasts. *J Hum Evol* 101, 65–78.

Beaudet A, Dumoncel J, Bam L, et al. (2016b) Reconstructing early hominin brain evolution from South African *Australopithecus* endocasts. *Am J Phys Anthropol Suppl* 62, 89 (abstract).

Berger LR, Hawks J, de Ruiter DJ, et al. (2015) Homo naledi, a new species of the genus Homo from the Dinaledi Chamber, South Africa. *eLife*, 4, e09560. doi: 10.7554/eLife.09560.

Besl PJ, McKay ND (1992) A method for registration of 3-D shapes. *IEE Trans Pattern Anal* 14(2), 239–256.

Broom R (1947) Discovery of a new skull of the South African ape-man, *Plesianthropus. Nature* 159, 672.

Broom R, Schepers GWH (1946) *The South African Fossil Ape-Men: the Australopithecinae*. Transvaal Museum Memoir No. 2. Pretoria: Transvaal Museum.

Brown P, Sutikna T, Morwood MJ, et al. (2004) A new smallbodied hominin from the Late Pleistocene of Flores, Indonesia. *Nature* 431, 1055–1061.

Bruner E, Manzi G, Arsuaga JL (2003) Encephalization and allometric trajectories in the genus Homo: evidence from the Neandertal and modern lineages. *Proc Natl Acad Sci USA* 100, 15 335–15 340.

Carlson KJ, Stout D, Jashashvili T, et al. (2011) The endocast of MH1, *Australopithecus sediba. Science* 333, 1402–1407.

Conroy GC, Vannier MW, Tobias PV (1990) Endocranial features of *Australopithecus africanus* revealed by 2- and 3-D computed tomography. *Science* 247, 838–841.

Conroy GC, Weber GW, Seidler H, et al. (1998) Endocranial capacity in an early hominid cranium from Sterkfontein, South Africa*. Science* 280, 1730–1731.

Dart RA (1925) *Australopithecus africanus*: the man-ape of South Africa. *Nature* 115, 195–199.

Dray S, Dufour AB (2007) The ade4 package: implementing the duality diagram for ecologists. *J Stat Softw* 22, 1–20.

Dumoncel J, Durrleman S, Braga J, et al. (2014) Landmark-free 3D method for comparison of fossil hominins and hominids based on endocranium and EDJ shapes*. Am J Phys Anthropol* 153(Suppl. 56), 110.

Dumoncel J, Subsol G, Durrleman S, et al. (2016) How to build an average model when samples are variably incomplete? Application to fossil data. IEEE Conference on Computer Vision and Pattern Recognition (CVPR) Workshops, Las Vegas, USA, July 1, pp. 541–548.

Durrleman S (2010) Statistical models of currents for measuring the variability of anatomical curves, surfaces and their evolution. PhD thesis. Universit_e Nice-Sophia Antipolis, Nice.

Durrleman S, Pennec X, Trouv_e A, et al. (2012a) Comparison of the endocranial ontogenies between chimpanzees and bonobos via temporal regression and spatiotemporal registration. *J Hum Evol* 62, 74–88.

Durrleman S, Prastawa M, Korenberg JR, et al. (2012b) Topology preserving atlas construction from shape data without correspondence using sparse parameters. In: *Medical Image Computing and Computer-Assisted Intervention*, Vol. 7512, Part III. (eds Ayache N, Delingette H, Golland P, Mori K), pp. 223–230. Heidelberg: Springer.

Durrleman S, Prastawa M, Charon N, et al. (2014) Morphometry of anatomical shape complexes with dense deformations and sparse parameters. *NeuroImage* 101, 35–49.

El Khoury M, Braga J, Dumoncel J, et al. (2014) The human semicircular canals orientation is more similar to the bonobos than to the chimpanzees. *PLoS ONE* 9, e93824. https://doi.org/10.1371/journal.pone.0093824.

Falk D (1980) A reanalysis of the South African australopithecine natural endocasts. *Am J Phys Anthropol* 53, 525–539.

Falk D (1983a) The Taung endocast: a reply to Holloway. *Am J Phys Anthropol* 60, 479–489.

Falk D (1983b) Cerebral cortices of East african early hominids. S*cience* 221, 1072–1074.

Falk D (2009) The natural endocast of Taung (*Australopithecus africanus*): insights from the unpublished papers of Raymond Arthur Dart. *Am J Phys Anthropol* 140, 49–65.

Falk D (2012) Hominin paleoneurology: where are we now? *Prog Brain Res* 195, 255–272.

Falk D (2014) Interpreting sulci on hominin endocasts: old hypotheses and new findings. *Front Hum Neurosci* 8, 134.

Falk D, Redmond JC Jr, Guyer J, et al. (2000) Early hominid brain evolution: a new look at old endocasts. J Hum Evol 38, 695–717.

Falk D, Hildebolt C, Smith K, et al. (2005) The brain of LB1, *Homo floresiensis. Science 308*, 242–245.

Finlay BL, Darlington RB (1995) Linked regularities in the development and evolution of mammalian brains. *Science* 268, 1578–1584.

Gabunia LK, Vekua Abesalom K, Lordkipanidze D, et al. (2000) Earliest Pleistocene hominid cranial remains from Dmanisi, Republic of Georgia: taxonomy, geological setting and age. *Science* 288, 1019–1025.

Gilissen E (2001) Structural symmetries and asymmetries in human and chimpanzee brains. In: *Evolutionary Anatomy of the Primate Cerebral Cortex*. (eds Falk D, Gibson KR), pp. 187–215. Cambridge: Cambridge University Press.

Gómez-Robles A, Hopkins D, Sherwood CC (2014) Modular structure facilitates mosaic evolution of the brain in chimpanzees and humans. *Nat Commun* 5, 4469.

Grimaud-Hervé D, Lordkipanidze D, de Lumley M-A, et al. (2006) Étude préliminaire des endocrânes de Dmanissi: D 2280 et D 2282. L'Anthropologie 5, 732–765.

Gunz P, Neubauer S, Maureille B, et al. (2010) Brain development after birth differs between Neanderthals and modern humans. *Curr Biol* 20, 921–922.

Hager R, Lu L, Rosen GD, et al. (2012) Genetic architecture supports mosaic brain evolution and independent brain-body size regulation. *Nat Commun* 3, 1079.

Holloway RL (1972) New australopithecine endocast, SK 1585, from Swartkrans, South Africa. *Am J Phys Anthropol* 37, 173–185.

Holloway RL (1980) Stereoplotting hominid brain endocasts: some preliminary results. In: *NATO Symposium on Applications of Human Biostereometrics*, Vol. 166. (eds Coblentz AM, Herron RE), pp. 200–206. Bellingham: Proceedings of SPIE.

Holloway RL (1981) Revisiting the South African Taung australopithecine endocast: the position of the lunate sulcus as determined by the stereoplotting technique. *Am J Phys Anthropo*l 56, 43–58.

Holloway RL (1983) Human brain evolution: a search for units, models, and synthesis. *Can J Anthropol* 3, 215–232.

Holloway RL (2001) Does allometry mask important brain structure residuals relevant to species-specific behavioural evolution? *Behav Brain Sci* 24, 286–287.

Holloway RL, Clarke RJ, Tobias PV (2004a) Posterior lunate sulcus in *Australopithecus africanus*: was Dart right? *CR Palevol* 3, 1–7.

Holloway RL, Broadfield DC, Yuan MS (2004b) *The Human Fossil Record: Brain Endocasts, the Paleoneurological Evidence*. Hoboken: Wiley-Liss.

Holloway RL, Hurst SD, Garvin HM, et al. (2017) *Homo naledi* posterior endocasts and their significance for understanding brain reorganization. *Am J Phys Anthropol Suppl* 64, 220.

Hurst SD, Holloway RL, Garvin HM, et al. (2017) *Homo naledi's* frontal lobe: modern in form, ancestral in size. *Am J Phys Anthropol Suppl* 64, 225.

Kubo D, Kono RT, Kaifu Y (2013) Brain size of *Homo floresiensis* and its evolutionary implications. *Proc R Soc B* 280, 20130338.

Lee SH (2005) Is variation in the cranial capacity of the Dmanisi sample too high to be from a single species? *Am J Phys Anthropol* 127, 263–266.

Lieberman DE, Ross CF, Ravosa MJ (2000) The primate cranial base: ontogeny, function, and integration. *Yearb Phys Anthropol* 43, 117–169.

Lieberman DE, McBratney BM, Krovitz G (2002) The evolution and development of cranial form in *Homo sapiens. Proc Natl Acad Sci USA* 99, 1134–1139.

Lordkipanidze D, Ponce de Le_on MS, Margvelashvili A, et al. (2013) A complete skull from Dmanisi, Georgia, and the evolutionary biology of early *Homo. Science* 342, 326–331.

Mitteroecker P, Bookstein FL (2011) Linear discrimination, ordination, and the visualization of selection gradients in modern morphometrics. *Evol Biol* 38, 100–114.

Neubauer S, Gunz P, Hublin JJ (2010) Endocranial shape changes during growth in chimpanzees and humans: a morphometric analysis of unique and shared aspects. *J Hum Evol* 59, 555–566.

Neubauer S, Gunz P, Weber GW, et al. (2012) Endocranial volume of *Australopithecus africanus:* new CT-based estimates and the effects of missing data and small sample size. *J HumEvol* 62, 498–510.

Spoor CF (1997) Basicranial architecture and relative brain size of Sts 5 (*Australopithecus africanus*) and other Plio-Pleistocene hominids. *S Afr J Sci* 93, 182–186.

Spoor F, Jeffery N, Zonneveld F (2000) Using diagnostic radiology in human evolutionary studies. *J Anat* 197, 61–76.

Subsol G, Gesqui_ere G, Braga J, et al. (2010) 3D automatic methods to segment 'virtual' endocasts: state of the art and future directions. *Am J Phys Anthropol Suppl*. 50, 226–227.

Tallman M, Amenta N, Delson E, et al. (2014) Evaluation of a new method of fossil retrodeformation by algorithmic symmetrization: crania of papionins (Primates, Cercopithecidae) as a test case*. PLoS ONE* 9, e100833,https://doi.org/10.1371/journal.pone.0100833.

Tobias PV (1991*) The Skulls, Endocasts and Teeth of Homo habilis*. Olduvai Gorge, Vol .IV. Cambridge, England: Cambridge University Press.

de Winter W, Oxnard CE (2001) Evolutionary radiations and convergences in the structural organization of mammalian brains. *Nature* 409, 710–714.